Materials Displaying Neural Growth Factor Gradients and Applications in Neural Differentiation of Embryoid Body Cells

*Bahman Delalat, Agnieszka Mierczynska, Soraya Rasi Ghaemi, Alex Cavallaro, Frances J. Harding, Krasimir Vasilev, and Nicolas H. Voelcker**

The critical growth factor density required to support neural lineage generation from mouse embryonic stem cells is assessed by constructing a surface density gradient of immobilized nerve growth factor (NGF) from a plasma polymer film base. A chemical surface gradient varying from high hydroxyl group density to high aldehyde group density is prepared through diffusion-controlled plasma polymerization of two monomers (ethanol and propionaldehyde) under a moving mask. NGF density gradients are then produced by reductive amination with the aldehyde groups on the plasma polymer surface. Mouse embryoid body derived (mEB) cell differentiation on the gradient surface is evaluated by immunofluorescence staining against Nestin. mEB cell density and the percentage of Nestin-positive cells increase with increasing NGF density up to a critical value corresponding to 52.9 ng cm^{-2}, above which cell attachment and differentiation do not increase further. This gradient-based screening approach allows the growth factor surface densities to be optimized for biomaterials intended for cell differentiation or expansion, which is highly relevant to creating efficient manufacture processes for cell therapies.

1. Introduction

The interactions between cells and material surfaces can be improved significantly by the surface display of bioactive molecules. Biomolecules such as extracellular matrix (ECM) proteins, growth factors, glycosaminoglycans, and cell adhesion molecules have been widely exploited to bolster surface bioactivity and enable control over cell function.[1] One of the key applications for this capability is in the area of cell therapy. Competent ex vivo expansion of cells is a major requirement for the generation of clinical grade cells en mass. Versatile, cost efficient, robust, culture models, able to be scaled up using chemically characterized materials, must be developed to achieve this goal. Materials able to induce the appropriate cell behavior, be it expansion or differentiation, will become a cornerstone of cell therapy manufacture protocols.[2,3] Scale-up of cell manufacturing processes has been limited by the prohibitive expense associated with growth factor supplementation of culture medium. Critical for the control of cell differentiation and survival, the use of trophic factors in large scale processes is beset by their short life time in cell culture environments and the massive amounts needed to dose industrial volumes.[4] Previous research has established that immobilized growth factors modulate cell function in the same way as their soluble forms.[5] Through inhibition of endocytosis, the immobilization of growth factors has been reported to modify the apparent activity and half-life.[6] Thus immobilization on cell culture substrates may reduce the amount of growth factor required to elicit specific behaviors and, additionally, prolong its activity.[7] However, the expense associated with the amount of growth factor required to support stem cell maintenance and differentiation remains high even when immobilized, driving up the cost of such bioactive surface-engineered materials and potentially making them economically unviable.[8] Therefore, methods which allow us to identify the minimum density of surface-displayed biomolecules to evoke an appropriate cell response are in high demand.[9] This is a task well suited to surface-bound gradients, which have emerged as powerful platforms for high throughput screening of cell–material–surface interactions.[10–12] Surface-bound gradients have yet to be exploited to quantify the density of factor required to support embryonic stem cell (ESC) differentiation.

Plasma polymerization is an engineering-friendly and robust surface coating technique which has been successfully applied to functionalization of cell and tissue culture surfaces.[12] Plasma polymers provide pinhole-free and well-adherent coatings of controlled thickness on a wide range of substrate materials.[13] A plethora of functional groups including amines, carboxylic acids, aldehydes, and epoxy groups can be formed, with tuneable density.[12,14,15] Depending on the monomer composition, surface functionalization by plasma polymerization

Dr. B. Delalat, Dr. A. Mierczynska, S. Rasi Ghaemi, A. Cavallaro, Dr. F. J. Harding, Prof. K. Vasilev, Prof. N. H. Voelcker
Mawson Institute
University of South Australia
Mawson Lakes, SA 5095, Australia
E-mail: Nico.Voelcker@unisa.edu.au
Dr. A. Mierczynska
Ian Wark Research Institute
University of South Australia
Mawson Lakes, SA 5095, Australia

DOI: 10.1002/adfm.201500595

has been used to either promote or reduce protein adsorption and cell attachment.[14–16] The process of plasma polymerization is also compatible with the fabrication of chemical composition gradients, as several groups including our own have previously reported.[17] One approach to construct a plasma polymer gradient is to change the composition of the monomer gas feed entering the plasma chamber whilst moving the substrate mounted on a motorized stage under a slot in a shadow mask.[15] The advantage of this approach is that it affords control over the steepness and profile of the gradient, in contrast to other common approaches.[15] The resulting plasma polymer gradients allow the quantitative and high-throughput assessment of the relative cell attachment, proliferation, and differentiation along the direction of the gradient.[10,12,17,18]

Neurotrophic factors such as neutrophins are required for the growth and development of neurons.[19,20] As a result, they have been explored for their therapeutic potential in neuroprotection and regulation of neuron survival and differentiation.[21] Nerve growth factor (NGF) is the most common and well defined of the neurotrophins. This factor acts by repressing apoptosis, controlling morphogenesis, and survival synaptic functions of neurons.[22] NGF has been found to be of considerable therapeutic value for the treatment of degenerative disorders and damaged nerve tissue.[23] The fabrication of biomaterials incorporating immobilized NGF has been reported to successfully induce neuronal cell differentiation and stimulate neurite formation.[2,24–27] Biomaterials that display NGF on their surface evidently provide an improved environment for neurite outgrowth in nerve regeneration, particularly since damaged tissues do not provide adequate levels of neurotrophins.[28] Surface-immobilized NGF induces the activation of intracellular signaling cascades and thereby stimulates neurons without internalization in the process.[19,25] Surface immobilization via amino groups has been reported to retain higher levels of bioactivity than immobilization via other terminal groups.[26] Consequently, the stable bioconjugation of NGF on surfaces appears to integrate the signaling and biochemical cues required for nerve repair, but the question of what density of immobilized NGF is required to achieve the desired effect remains unanswered.[19]

A number of noncovalent modification strategies including doping and entrapping of ECM proteins or growth factors into biomaterials have been pursued in other differentiation contexts.[27,29] However, these techniques usually require a high concentration of factors. The other drawback of noncovalent modification techniques relates to the leaching of the factor from the biomaterial prior to tissue regeneration. As a result, covalent factor immobilization is preferred when designing tissue engineering scaffolds or tissue culture materials for cell expansion.[25,30]

The purpose of this study was to test the hypothesis that induction with covalently immobilized NGF will induce differentiation of mouse embryoid body derived (mEB) cells toward the neuronal lineage, allowing the optimum surface density of NGF to be determined. We employed surface-bound gradients to screen for attachment, proliferation, and differentiation of neural cell populations derived from mEB cells across a substrate with linearly increasing NGF density. To generate the NGF density gradient, we harnessed the plasma polymer gradient format, in this case using a gradient of aldehyde functional group density onto which NGF was covalently coupled by means of reductive amination. Plasma polymer coatings can be easily scaled up and transferred onto porous scaffolds or tissue cultureware.[31] Therefore, our work has direct implications for the design of advanced nerve tissue engineering scaffolds and tissue culture surfaces for neural cell expansion.

2. Results and Discussion

2.1. Generation of Plasma Polymer Gradients and Surface Analysis

Propionaldehyde and ethanol monomers were selected for the generation of the plasma polymer gradient that forms the base layer template for the NGF surface gradient test surface. Propionaldehyde and ethanol are both good candidates for plasma polymerization since they are easy to vaporize. Ethanol plasma polymers are reasonably inert and non-fouling, whilst the aldehyde functional groups present in propionaldehyde plasma polymer are chemically reactive to amine groups.[14] Hence, propionaldehyde plasma polymers or plasma polymers made from monomer mixtures including propionaldehyde can be used for one step immobilization of biomolecules.[32,33]

Thin plasma polymer gradients progressing from ethanol plasma polymer to propionaldehyde plasma polymer over a 13 mm distance were prepared on glass coverslips using plasma co-polymerization of the two monomers while moving a shadow mask with a slit over the substrate and simultaneously modifying the ratio of ethanol and propionaldehyde vapor feed. The resulting gradient samples were analyzed via x-ray photoelectron spectroscopy (XPS). Typical C1s high-resolution spectra recorded near the ethanol plasma polymer end (position 1 mm) and the propionaldehyde plasma polymer ends (position 12 mm) of the gradient are shown in **Figure 1**A,B. Peak deconvolution analysis demonstrated the presence of four carbon bonded chemical groups within the plasma polymer films: aliphatic hydrocarbons (C—H) at 285.0 eV, single bonded oxygen-carbons (C—O) at 286.5 eV, double bonded oxygen-carbons (C═O) at 288.0 eV and ester/carboxyl functionalities at 289.0 eV. The spectra clearly show higher amount of C═O bonds on the aldehyde rich end of the gradient. The percentage of C═O functionalities across the surface are shown in Figure 1C. The data reveal an increase of C═O content toward the aldehyde-rich end of the gradient (position 12 mm) which is consistent with our earlier studies.[15] Additional characterization of the plasma polymer gradient surface revealed no appreciable change in surface roughness or film thickness. Likewise, water contact angle did not change across the gradient (Supporting Information, Figures S1 and S2).

2.2. Quantification of Immobilized NGF Density on Gradient Surfaces

To translate the aldehyde functional group gradient surface into a gradient of NGF density, we covalently bound the

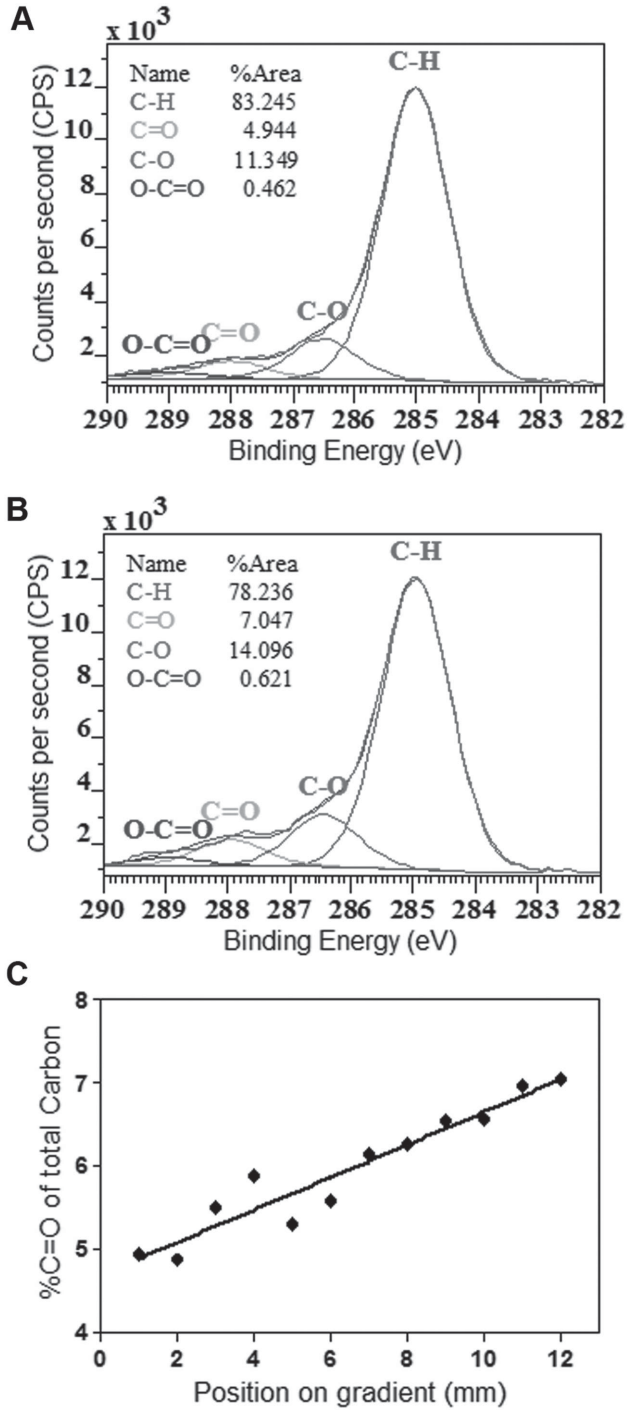

Figure 1. High-resolution C1s spectra obtained from XPS at the ethanol A) and propionaldehyde plasma polymer B) end of the gradient. Outlined areas represent individual peaks of C—H (purple), C—O(red), C═O (light blue), and O—C═O (dark blue). C) Relative concentration of C═O along the gradient from the ethanol plasma polymer to the propionaldehyde plasma polymer end.

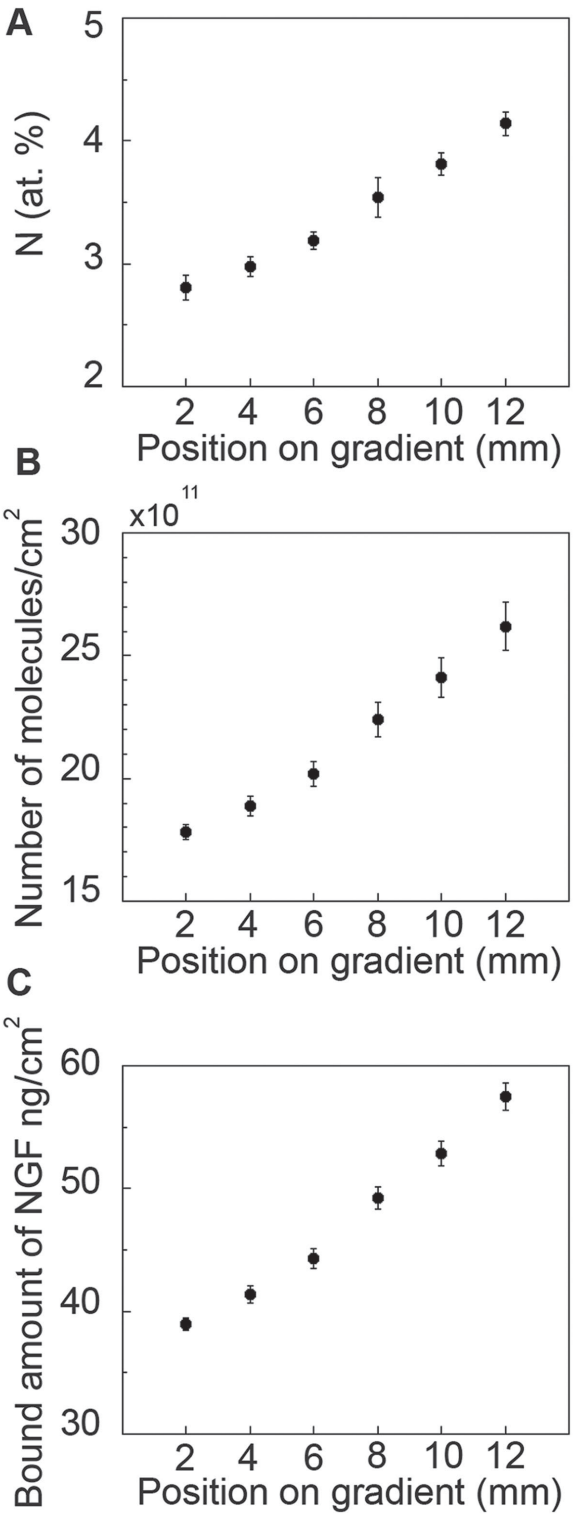

Figure 2. Quantification of the surface density of NGF on an ethanol-propionaldehyde plasma polymer gradient via XPS. A) The nitrogen percentage of NGF immobilized via reductive amination on ethanol-propionaldehyde plasma polymer gradient surface. Error bars correspond to standard error; $n = 3$. B) The number of NGF molecules per cm^2 along the NGF gradient surface was calculated as explained in the Supporting Information. C) The bound amount was calculated by converting the number of NGF molecules per cm^2 to the amount of NGF per cm^2.

growth factor to aldehyde functional groups using reductive amination chemistry.[15,33] The ethanol plasma polymer is known to adsorb only minimal amounts of protein.[14,15] Two types of substrates were created: one employing a weak and

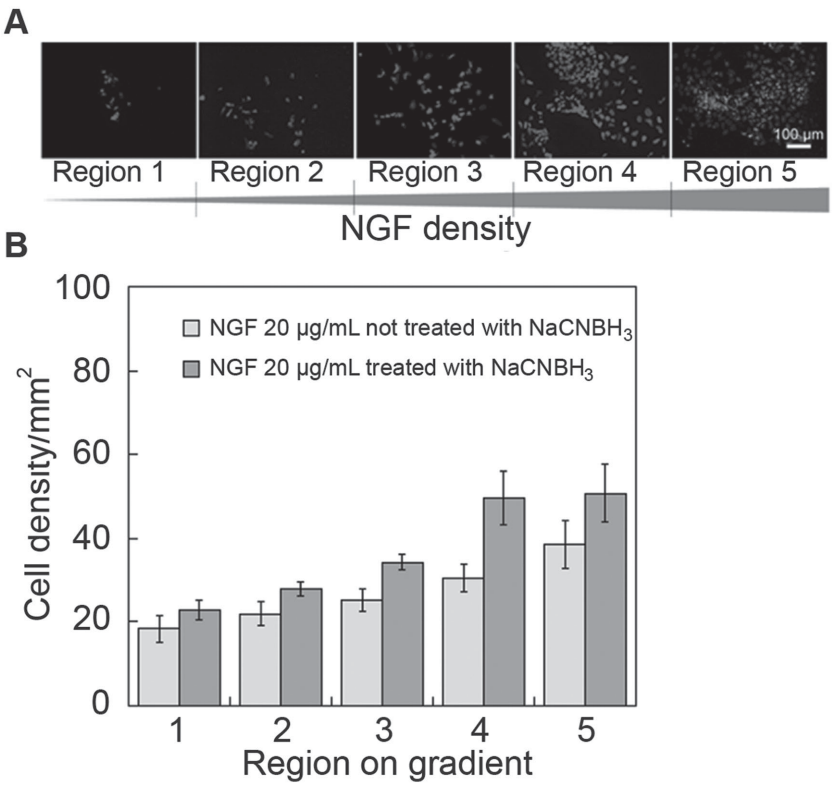

Figure 3. A) Representative mEB cell fluorescence microcopy images along the NGF gradient surface after 12 h incubation. Cell nuclei were stained with Hoechst 33342. B) Total cell attachment (averaged per mm^2) determined by a cell count in each region of the NGF gradient surface after 12 h incubation. Error bars correspond to standard error; $n = 3$.

reversible covalent link (a Schiff base) to immobilize NGF, the other using an irreversible amine bond (upon addition of $NaCNBH_3$ as a reducing agent during NGF immobilization). NGF immobilized without $NaCNBH_3$ would be expected to detach from the surface when exposed to aqueous culture environments.

The amount of immobilized protein across NGF gradients fabricated using reductive amination was determined using XPS measurements. **Figure 2**A shows the atomic percentage of nitrogen at six positions along the surface. Note that the plasma polymer chemical gradient itself does not contain any nitrogen.[15] Thus, the nitrogen signal detected on the surface can be attributed to immobilized NGF. As can be seen from Figure 2A, the atomic concentration of nitrogen increases linearly ($R^2 = 0.99$), by a total of ≈1.5 fold, toward the aldehyde plasma polymer functional group rich end of the gradient. These results are consistent with our earlier work generating functional surface gradients of streptavidin surface density.[15] Knowledge of the nitrogen concentration allowed us to calculate the number of protein molecules per square centimeter across the gradient via a correlation of quartz crystal microbalance with dissipation (QCM-D) data and XPS data (Supporting Information).[15] Figure 2B shows that the density of protein molecules immobilized increased from 17.8×10^{11} to 26.2×10^{11} molecules cm^{-2} when the propionaldehyde plasma polymer was at the highest density on the gradient. The surface density of immobilized NGF gradually increased linearly from 39 to 57.5 ng cm^{-2} over a distance of 10 mm (Figure 2C). Without reductive amination, the gradient of NGF surface density produced is much shallower. NGF surface density is similar in the Schiff base and reduced gradients at the ethanol plasma polymer (low) end (Supporting Information, Figure S3). Higher NGF surface density is evident in the $NaCNBH_3$ treated gradients compared to untreated controls from the 4 mm position onwards. At the propionaldehyde plasma polymer-rich end of the gradients, the density of NGF is 35% higher on reduced gradients compared to Schiff base control gradients.

2.3. mEB Cell Response to NGF Gradient Surfaces

Cell attachment and proliferation on NGF gradient surfaces was studied with mEB cells grown in complete medium. The gradient surface was divided into five equally sized zones of steadily increasing NGF density. We first investigated the influence of immobilized growth factor density on attached cell density. The mEB cell attachment after 12 h incubation on the NGF gradient is presented in **Figure 3**. Cell density increased from region 1 to region 4 and then reached a plateau. When the reducing agent ($NaCNBH_3$) required for reductive amination was not added during NGF immobilization (in which case an unstable Schiff base is constituted between amines on the NGF and the aldehyde on the surface), cell density was consistently lower than gradients of covalently bound NGF constructed using reductive amination, and cell density increased along the gradient from region 1 to region 5. It should be noted that only a few cells attached to an ethanol-propionaldehyde plasma polymer gradient without NGF or to a bare coverslip. After 2–3 d, these few cells had already detached from the surface.

We next investigated mEB cell proliferation on the gradient surfaces over the course of one week (**Figure 4**). Across the gradient surface, mEB cell density increased over this time frame. The growth rate of cells increased with increasing density of immobilized NGF until region 4 and then remained stable (Figure 4A). Cell density increased 2.2-fold on regions 4 and 5 compared to 1.5-fold on region 1 over the course of 7 d. Cells proliferated more rapidly on the regions (4 and 5) compared to the regions with lower density of NGF. On the NGF gradient surfaces where $NaCNBH_3$ was omitted, an increase in cell density was observed to correlate with NGF surface density, but this was not statistically significant. Overall, cell proliferation was lower (1.5-fold increase in density over 7 d in region 5) than on the gradients where NGF was covalently attached via reductive amination (Figure 4B).The difference between the two types of surfaces can be explained by the NGF bound via a Schiff base desorbing

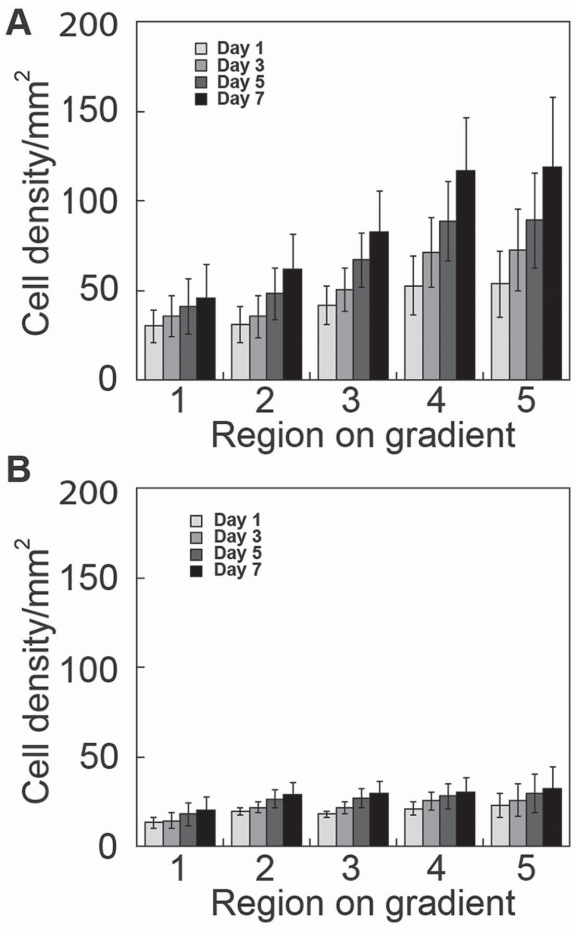

Figure 4. A) Cell proliferation (averaged per mm^2) on NGF gradient with $NaCNBH_3$ treatment determined by cell counts at each region from day 1, every 48 h over the course of 7 d. Cell seeding density was 1×10^4 cell mL^{-1}. Error bars correspond to standard error. B) Cell proliferation on NGF gradient not treated with $NaCNBH_3$. Error bars correspond to standard error; $n = 3$.

over the course of the experiments and being diluted in cell culture medium.

2.4. Differentiation of EB Cells into Neuroepithelial Cells

The above results show that changes in NGF density and the mode of NGF attachment influence the attachment and proliferation of mEB cells. Next, we investigated whether the immobilized growth factor density also influenced mEB differentiation toward neural lineages by using the neuroepithelial cell marker protein Nestin (NES), expressed in neural stem cells.[34] NES expression was determined in mEB single cell suspensions before seeding on the gradient surface at day zero. At this timepoint, NES was not expressed in individual mEB cells. Cells grown on the NGF gradient for 7 d were fixed and stained with antibodies to NES (**Figure 5**A). Immunofluorescence examination revealed that the percentage of NES-positive cells increased from 38% at region 1 to around 98% at regions 4 and 5 (Figure 5B). Importantly, we found that the density of 52.9 ng cm^{-2} NGF on region 4 was sufficient to induce almost complete neural lineage differentiation. A further increase in NGF density (57.5 ng cm^{-2}, region 5) did not improve differentiation efficiency. Concurrent with the observed rise in NES expression, cell morphology developed an increasingly dendritic morphology on NGF rich regions of the gradient (Figure 5C).

In contrast, on gradient surfaces constructed without the addition of $NaCNBH_3$ during NGF immobilization, the percentage of nestin positive cells increased from 3% to 52% across the gradient. Within each region of this gradient, the numbers of nestin positive cells were lower compared to gradient surfaces created using the reducing agent to drive reductive amination (Figure 5D). In the absence of any NGF, gradient surfaces did not induce any NES expression in the overlying cells (Supporting Information, Figure S4). These results show that the irreversible covalent bonding of NGF to the surface improves neural cell formation. Existing studies have shown that NGF internalization is not required in order to affect cell behavior, therefore justifying the presentation of this growth factor in immobilized form.[26,35]

3. Conclusions

The immobilized biomolecule gradient format provides a versatile platform that is compatible with a range of cell-based assays and conducive to high throughput screening. In this study, surface-immobilized growth factor gradients were prepared by covalent attachment of NGF via reductive amination by $NaCNBH_3$ on ethanol/propionaldehyde plasma polymer gradients. The amount of immobilized NGF on the plasma polymerized gradient surface across the gradient was calculated using QCM-D data and XPS data. mEB cell behavior was studied across the NGF gradient. mEB cells experienced significant enhancements in attachment, proliferation, and neural differentiation up to an immobilized NGF density of 52.9 ng cm^{-2}. A further increase in NGF density did not convey a greater proliferation or differentiation stimulus. This study therefore provides a valuable lesson of how chemical gradients can be harnessed for biomaterial design. Our results provide new insights into the requirements for surface-displayed NGF density in order to stimulate mEB cells to differentiate to a neural lineage, which is highly relevant to nerve tissue engineering. In view of the high cost of growth factors, research into materials conducive to therapeutic cell expansion will benefit from this screening capability, which enables the minimization of the required growth factor densities and makes bioactive materials more affordable and accessible.

4. Experimental Section

Preparation of Ethanol-Propionaldehyde Plasma Polymer Gradients: Thin film polymeric gradients progressing from ethanol plasma polymer (monomer: absolute 99.5% v/v, Ajax Finechem) to propionaldehyde plasma polymer (monomer: reagent grade 97%, Sigma-Aldrich) were prepared on 13 mm glass coverslips by performing plasma co-polymerization of the two monomers while moving a shadow mask

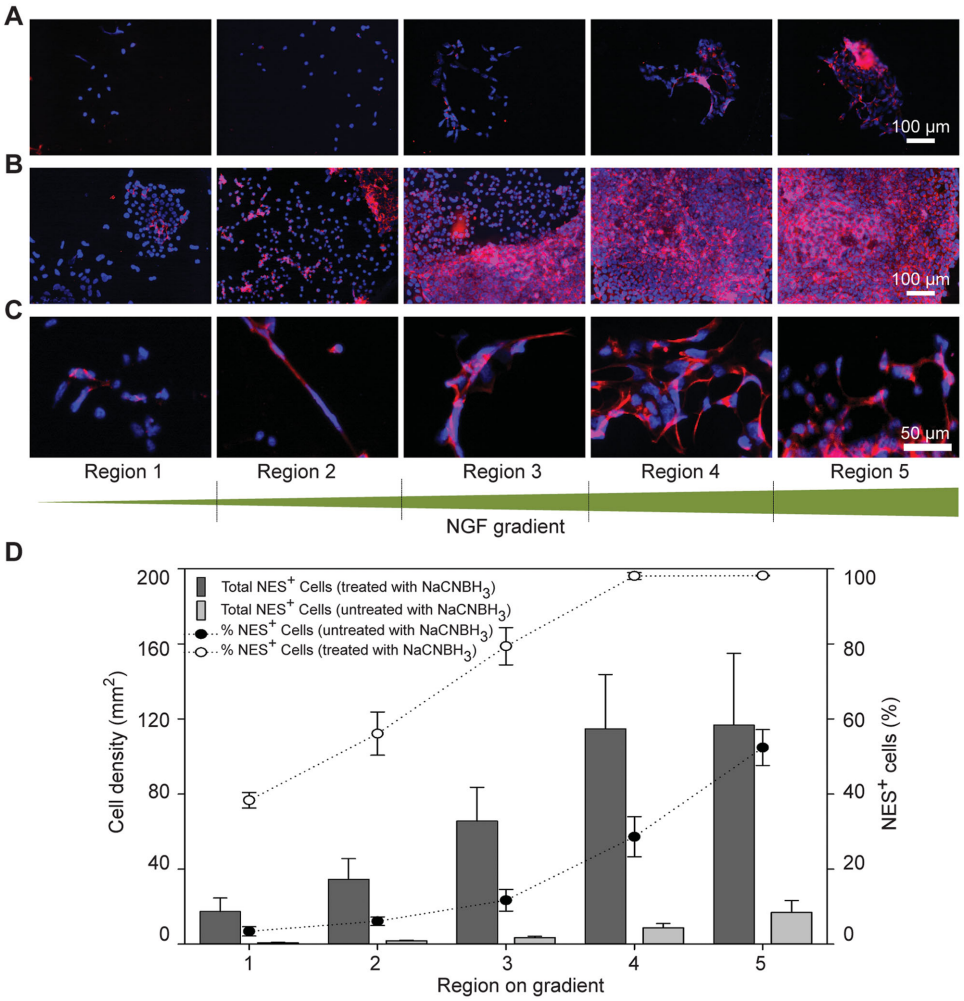

Figure 5. Immunofluorescence staining for neural lineage marker. A,B) Nestin staining (red) of mEB cells on the five regions of the NGF gradient surfaces is shown 7 d after seeding (scale bar = 100 μm) for A) not treated with $NaCNBH_3$ and B) with $NaCNBH_3$ treatment. Nuclei of cells were counterstained with Hoechst 33342 (blue). C) High resolution images of cells on each region showing changes in cell morphology. D) Quantification of neural lineage differentiation marker expression in mEB cells at each region on the gradient. Total NES+ cells per unit area in each region are shown in the bar chart (left-hand *y*-xis). The percentage of NES+ cells in each region are shown in line chart (right-hand *y*-axis). The error bars represent the standard error. Error bars correspond to standard error; $n = 3$.

with a uniform rate of 1 mm min^{-1} over the coverslip and simultaneously changing the ratio of ethanol and propionaldehyde vapor feed. The initial flow rate of ethanol vapor was 10 sccm which was linearly reduced to 0 sccm between the 6 and 12 mm positions along the gradient. Conversely, the flow rate of propionaldehyde vapor was linearly increased from 0 sccm at 6 mm to 10 sccm at 10 mm and remained at 10 sccm for the rest of the procedure. A custom-built gradient plasma apparatus operated with a 13.56 MHz radiofrequency generator using programmed valves was used as previously described.[11,36] Deposition throughout the entire process was carried out using a plasma power of 40 W.

Surface Characterization: XPS analysis was applied to identify the surface composition of the ethanol-propionaldehyde plasma polymer gradients. Twelve points along a 13 mm gradient were measured at 1 mm intervals. The origin of the gradient was defined as $x = 0$ mm and corresponds to the ethanol plasma polymer end. An XPS measurement could not be taken at the extreme ends of the gradient ($x = 0$ and 13 mm). Coated samples were characterized for their surface chemical compositions using a Kratos Axis Ultra delay-line detector spectrometer equipped with a monochromatic Al Kα source (1486.6 eV) operating at 10 kV and 13 mA, utilizing a spot size of 300 × 700 μm^2. The samples were analyzed at a pressure of 2×10^{-9} Torr at room temperature. Elements present in a sample surface were determined from the survey spectrum recorded over the energy range of 0–1125 eV at a pass energy of 120 eV. The areas under selected photoelectron peaks in a widescan spectrum were used to calculate percentage atomic concentrations. High-energy resolution C1s spectra were then recorded at 20 eV pass energy. All the binding energies (BEs) were referenced to the C1s neutral carbon peak at 285.0 eV, to compensate for the effect of surface charging. Individual components within the C1s spectra had set position constraints of 285.0 eV (CH), 286.5 eV (C—), 288.0 eV (C═), and 289.0 eV (COOR) and full width at half maximums (FWHM) of 1.1–1.4 eV, ensuring that all component FWHM matched the FWHM of the CH bond. The processing and curve-fitting of the high-energy resolution spectra were performed using CasaXPS software (ver. 2.3.14, Casa Software Ltd).

Covalent Immobilization of NGF onto Ethanol-Propionaldehyde Plasma Polymer Gradient Surfaces: Prior to incubation of NGF on the ethanol-propionaldehyde plasma polymer gradient surface, the coated coverslips were washed with copious amounts of sterile Dulbecco's phosphate-buffered saline solution (PBS) (Sigma) to remove any unbound plasma polymer. Then, the coverslips were sterilized with 200 U mL^{-1} penicillin, 200 μg mL^{-1} streptomycin and 500 ng mL^{-1} amphotericin B (Invitrogen)

in sterile PBS for 1 h and were washed three times in sterile PBS. NGF at concentration of 20 μg mL^{-1} in PBS was incubated on ethanol-propionaldehyde gradient surfaces for 16 h at 4 °C. After incubation, NGF solution was aspirated and washed two times with PBS solution followed by treatment with 0.05 M sodium cyanoborohydride ($NaCNBH_3$) for 4 h at room temperature. In order to block unreacted propionaldehyde sites, we added 0.06 M ethanolamine for 30 min at room temperature followed by treatment with $NaCNBH_3$. Prior to analysis by XPS, surfaces were washed with surfactant, 10% sodium dodecyl sulphate (BioRad), then rinsed thoroughly with copious amounts of Milli-Q water and thoroughly dried under a stream of nitrogen gas. Control surfaces that did not undergo reductive amination were treated in the same way prior to XPS. XPS enabled further characterization of the surface chemistry of the NGF gradient. Six different points at 2 mm intervals along a 13 mm gradient were mapped by XPS (positions from ethanol plasma polymer end of the gradient, $x = 0$ mm). The areas under the specific peaks were used to calculate the atomic percentages. Then, the amount of NGF binding was calculated from the percentage of nitrogen in NGF (see the Supporting Information).[14,15]

Preparation of mEB Cells: The D3 mouse ESC line (ATCC CRL1934) was maintained on a feeder layer of gamma irradiated STO-1 cells and incubated at 37 °C with 5% CO_2 in Advanced Dulbecco's modified Eagle's medium (DMEM) supplemented with 10% ESC qualified fetal bovine serum (FBS; Invitrogen), 10 ng mL^{-1} leukemia inhibitory factor (Millipore), 0.1×10^{-3} M β-mercaptoethanol (Sigma), 2×10^{-3} M L-glutamine, 100 U mL^{-1} penicillin, 100 g mL^{-1} streptomycin (Invitrogen), for 2–3 d until they were 70%–80% confluent. For mEB cell formation, ESC were dissociated with trypsin/EDTA solution and plated at density of 2.5×10^4 cells cm^{-2} onto non-adhesive petri dishes in Advanced DMEM, 10% FBS (Invitrogen), 0.1×10^{-3} M β-mercaptoethanol, 2×10^{-3} M L-glutamine, 100 U mL^{-1} penicillin, 100 μg mL^{-1} streptomycin. After 2 d in culture, ESCs aggregated into mEBs. The culture of mEBs continued for a further 6 d before single-cell suspensions of mEB cells were generated using 0.05% trypsin-0.53×10^{-3} M ethylenediaminetetraacetic acid (EDTA; Invitrogen). The cells were passed through a nylon mesh filter with pore size of 100 μm (BD Falcon) to obtain a single cell suspension. The viability of mEB cells was assessed before seeding onto the NGF gradient using Trypan blue staining.

mEB Culture on NGF Gradient Surfaces: Coverslip sample containing the NGF gradients were placed in 24-well plates (Nunc) and seeded with mEB cells at a density of 1×10^4 cells mL^{-1} per well in fresh cell culture medium. As controls, cells were also plated onto sterile round 13 mm glass coverslips ($n = 3$) and ethanol-propionaldehyde plasma polymer gradient coated coverslips ($n = 3$) at the same density. All mEB cells were cultured for 7 d in EB medium at 37 °C in a humidified atmosphere with 5% CO_2. To investigate the effects of the NGF gradient on mEB cell behavior, no other bioactive factors were added to the culture medium. The cell culture medium was changed every 2 d. Cytotoxicity assays of mEB cells on NGF gradient surfaces were performed by live-dead staining using a final concentration of 15 μg mL^{-1} fluorescein diacetate (Invitrogen) and 5×10^{-6} M propidium iodide (Sigma) in PBS for 3 min at 37 °C. Loosely attached cells were removed by rinsing with PBS ≈12 h after seeding. Gradients were divided into five equally broad regions of increasing NGF density (positions from ethanol plasma polymer rich end of the gradient: 0.0–2.6 mm = region 1, 2.6–5.2 mm = region 2, 5.2–7.8 mm = region 3, 7.8–10.4 mm = region 4, and finally 10.4–13 mm = region 5). Brightfield images of each region were acquired using an inverted light microscope (Olympus CK2) equipped with a Nikon Digital Sight DS-SM digital camera. The cell density on the gradient surfaces was evaluated by counting the number of attached cells within each region on each day for the first week of culture. Cell proliferation experiments were repeated three times on independent samples.

Neural Differentiation: The differentiation of mEB cells into the neural lineage was assessed via nestin immunofluorescence. Cultured cells were gently rinsed with PBS to remove culture media and serum proteins. The cells were fixed in 4% paraformaldehyde solution (Electron Microscopy Science) for 10 min. To allow the primary antibodies to enter the cells, the samples were rinsed again in PBS and then incubated in 0.1% Triton X-100 in PBS at room temperature for 5 min, then blocked with 10% serum from the species that the secondary antibody (donkey) was raised in PBS for 1 h. Immunofluorescence was performed by incubating the cells with goat antinestin monoclonal IgG (NES, Santa Cruz, diluted 1:200 in PBS) as a neural cell marker. After incubation with the primary antibodies for overnight at 4 °C and washing three times with PBS, the secondary antibody, phycoerythrin- (PE-) conjugated donkey anti-goat (Santa Cruz, diluted 1:100 in PBS), was added for 1 h at room temperature. Negative controls were carried out by eliminating the primary antibody labeling step from the procedure, which in all cases resulted in a complete loss of signal from fluorescence-labeled secondary antibodies. Finally, the nuclei were counterstained with 0.2 μg mL^{-1} Hoechst 33342 (Invitrogen) in PBS for 10 min, rinsed with PBS and mounted. Gradients were divided into five equal regions of gradually increasing NGF as per section 2.6, and cell behavior was compared between each zone. Images were obtained on a Nikon Eclipse Ti–S inverted fluorescence microscope equipped with a Nikon Digital Sight DS-2MBWc digital camera and NIS-Elements imaging software. Immunofluorescence analysis was repeated in three independent experiments. Nestin immunofluorescence was also performed on single-cell suspensions of mEB cells before seeding on NGF gradient surfaces in order to identify already differentiated cells.

Statistical Analysis: A one-way analysis of variance (ANOVA) analysis was carried out to quantify cell adhesion differences between the five gradient regions specified in Section 4.5, followed by post hoc analysis of means using the Tukey test. A p value of lower than 0.05 was considered statistically significant. Statistical investigations were conducted using KaleidaGraph software.

Supporting Information

Supporting Information is available from the Wiley Online Library or from the author.

Acknowledgements

Financial support from the South Australian Premier's Science and Research Fund is kindly acknowledged.

Received: February 11, 2015
Published online: March 25, 2015

[1] a) N. Gomez, Y. Lu, S. Chen, C. E. Schmidt, *Biomaterials* **2007**, *28*, 271; b) D. E. Discher, D. J. Mooney, P. W. Zandstra, *Science* **2009**, *324*, 1673; c) J. Venugopal, S. Low, A. T. Choon, S. Ramakrishna, *J. Biomed. Mater. Res., Part B* **2008**, *84*, 34; d) S. Rasi Ghaemi, F. J. Harding, B. Delalat, S. Gronthos, N. H. Voelcker, *Biomaterials* **2013**, *34*, 7601; e) S. B. Rønning, M. E. Pedersen, P. V. Andersen, K. Hollung, *Differentiation* **2013**, *86*, 13.

[2] M. Nakajima, T. Ishimuro, K. Kato, I.-K. Ko, I. Hirata, Y. Arima, H. Iwata, *Biomaterials* **2007**, *28*, 1048.

[3] a) A. M. Ross, J. Lahann, *J. Polym. Sci., Part B: Polym. Phys.* **2013**, *51*, 775; b) M. P. Lutolf, P. M. Gilbert, H. M. Blau, *Nature*, *462*, 433.

[4] a) J. L. Venero, F. Hefti, B. Knusel, *Mol. Pharmacol.* **1996**, *49*, 303; b) H. Brem, M. Klagsbrun, in *Oncogenes and Tumor Suppressor Genes in Human Malignancies* (Eds: C. C. Benz, E. T. Liu), Kluwer Academic Publishers, Boston, MA **1993**, Ch. 10; c) D. Giri, F. Ropiquet, M. Ittmann, *Clin. Cancer Res.* **1999**, *5*, 1063; d) L. Hwang, B.-F. Chen, P.-J. Lee, S. Ho, J. Liu, *Biotechnol. Appl. Biochem.* **1992**, *16*, 171; e) J. Mythili, S. Padmavathy, G. Chandrakasan, *Biotechnol. Appl. Biochem.* **2001**, *34*, 33; f) L. De Bartolo, A. Bader, *Biomaterials for Stem Cell Therapy:*

State of Art and Vision for the Future, CRC Press, Boca Raton, FL **2013**.
[5] M. Ghaedi, N. Tuleuova, M. A. Zern, J. Wu, A. Revzin, *Biochem. Biophys. Res. Commun.* **2011**, *407*, 295.
[6] K. Miyazawa, D. Williams, A. Gotoh, J. Nishimaki, H. Broxmeyer, K. Toyama, *Blood* **1995**, *85*, 641.
[7] a) Y. J. Park, K. H. Kim, J. Y. Lee, Y. Ku, S. J. Lee, B. M. Min, C. P. Chung, *Biotechnol. Appl. Biochem.* **2006**, *43*, 17; b) M. R. Doran, B. D. Markway, I. A. Aird, A. S. Rowlands, P. A. George, L. K. Nielsen, J. J. Cooper-White, *Biomaterials* **2009**, *30*, 4047.
[8] M. G. Ortore, R. Sinibaldi, P. Heyse, S. Paulussen, S. Bernstorff, B. Sels, P. Mariani, F. Rustichelli, F. Spinozzi, *Appl. Surf. Sci.* **2008**, *254*, 5557.
[9] a) S. Tang, J. Zhu, Y. Xu, A. P. Xiang, M. H. Jiang, D. Quan, *Biomaterials* **2013***34*, 7086; b) A. Rachkov, Y. Holodova, Y. Ushenin, D. Miroshnichenko, G. Telegeev, A. Soldatkin, *Sens. Lett.* **2009**, *7*, 957.
[10] F. J. Harding, L. R. Clements, R. D. Short, H. Thissen, N. H. Voelcker, *Acta Biomater.* **2012**, *8*, 1739.
[11] K. Vasilev, A. Mierczynska, A. L. Hook, J. Chan, N. H. Voelcker, R. D. Short, *Biomaterials* **2010**, *31*, 392.
[12] F. Harding, R. Goreham, R. Short, K. Vasilev, N. H. Voelcker, *Adv. Healthcare Mater.* **2012**, *8*, 1739.
[13] a) K. Vasilev, A. Michelmore, H. J. Griesser, R. D. Short, *Chem. Commun.* **2009**, 3600; b) K. Vasilev, A. Michelmore, P. Martinek, J. Chan, V. Sah, H. J. Griesser, R. D. Short, *Plasma Processes Polym.* **2010**, *7*, 824.
[14] B. R. Coad, T. Scholz, K. Vasilev, J. D. Hayball, R. D. Short, H. J. Griesser, *ACS Appl. Mater. Interfaces* **2012**, *4*, 2455.
[15] B. R. Coad, K. Vasilev, K. R. Diener, J. D. Hayball, R. D. Short, H. J. Griesser, *Langmuir* **2012**, *28*, 2710.
[16] D. B. Haddow, D. A. Steele, R. D. Short, R. A. Dawson, S. Macneil, *J. Biomed. Mater. Res., Part A* **2003**, *64A*, 80.
[17] a) A. Michelmore, L. Clements, D. A. Steele, N. H. Voelcker, E. J. Szili, *J. Nanomater.* **2012**, *2012*, 8; b) M. Zelzer, R. Majani, J. W. Bradley, F. R. Rose, M. C. Davies, M. R. Alexander, *Biomaterials* **2008**, *29*, 172.
[18] J. Genzer, *Annu. Rev. Mater. Res.* **2012**, *42*, 435.
[19] L. M. Yu, F. D. Miller, M. S. Shoichet, *Biomaterials* **2010**, *31*, 6987.
[20] K. Bartkowska, K. Turlejski, R. L. Djavadian, *Acta Neurobiol. Exp.* **2010**, *70*, 454.
[21] a) C.-H. Hung, Y.-C. Li, T.-H. Young, *BME* **2013**, *25*, 1; b) H. Wang, X. Duan, Y. Ren, Y. Liu, M. Huang, P. Liu, R. Wang, G. Gao, L. Zhou, Z. Feng, *Mol. Neurobiol.* **2013**, *47*, 24; c) I. Tasset, F. Medina, I. Jimena, E. Agüera, F. Gascon, M. Feijóo, F. Sánchez-López, E. Luque, J. Peña, R. Drucker-Colín, *Neuroscience* **2012**, *209*, 54; d) J.-P. Yang, H.-J. Liu, H. Yang, P.-Y. Feng, *Neurol. Sci.* **2011**, *32*, 433.
[22] a) J. Arikkath, *Front. Cell. Neurosci.* **2012**, *6*, 1; b) R. Levi-Montalcini, *Prog. Brain Res.* **1976**, *45*, 235; c) E. M. Shooter, *Annu. Rev. Neurosci.* **2001**, *24*, 601.
[23] M. J. O'Neill, T. K. Murray, M. P. Clay, T. Lindstrom, C. R. Yang, E. S. Nisenbaum, *CNS Drug Rev.* **2005**, *11*, 77.
[24] a) M. H. Chen, P. R. Chen, M. H. Chen, S. T. Hsieh, F. H. Lin, *J. Biomed. Mater. Res., Part A* **2006**, *79*, 846; b) J. Y. Lee, J.-W. Lee, C. E. Schmidt, *J. R. Soc. Interface* **2009**, *6*, 801; c) C. Chun, J. J. Hickman, W. Wang, C. Gregory, S. Narayanan, M. Poeta, presented at Conf. 24th Army Sci., Orlando, November **2004**; d) Y. Cho, R. Shi, A. Ivanisevic, R. B. Borgens, *Nanotechnology* **2009**, *20*, 275102; e) T. W. Chung, D. M. Lai, S. D. Chen, Y. I. Lin, *J. Biomed. Mater. Res., Part A* **2013**, *102*, 315; f) T. A. Kapur, M. S. Shoichet, *J. Biomed. Mater. Res., Part A* **2004**, *68*, 235; g) S. C. Park, S. H. Oh, J. H. Lee, *TERM* **2011**, *8*, 192.
[25] N. Gomez, C. E. Schmidt, *J. Biomed. Mater. Res., Part A* **2007**, *81*, 135.
[26] E. K. Yim, K. W. Leong, *J. Biomater. Sci. Polym. Ed.* **2005**, *16*, 1193.
[27] K. Moore, M. Macsween, M. Shoichet, *Tissue. Eng.* **2006**, *12*, 267.
[28] a) J. G. Boyd, T. Gordon, *Mol. Neurobiol.* **2003**, *27*, 277; b) G.-Z. Jin, M. Kim, U. S. Shin, H.-W. Kim, *Neurosci. Lett.* **2011**, *501*, 10.
[29] I. C. Bonzani, J. H. George, M. M. Stevens, *Curr. Opin. Chem. Biol.* **2006**, *10*, 568.
[30] H.-K. Song, B. Toste, K. Ahmann, D. Hoffman-Kim, G. Palmore, *Biomaterials* **2006**, *27*, 473.
[31] F. Intranuovo, E. Sardella, R. Gristina, M. Nardulli, G. Ceccone, P. Favia, R. d'Agostino, *Bone* **2008**, *15*, 16.
[32] a) K. S. Siow, L. Britcher, S. Kumar, H. J. Griesser, *Plasma Processes Polym.* **2006**, *3*, 392; b) T. M. Blättler, S. Pasche, M. Textor, H. J. Griesser, *Langmuir* **2006**, *22*, 5760.
[33] K. R. Diener, S. N. Christo, S. S. Griesser, G. T. Sarvestani, K. Vasilev, H. J. Griesser, J. D. Hayball, *Acta Biomater.* **2012**, *8*, 99.
[34] D. Park, A. P. Xiang, F. F. Mao, L. Zhang, C. G. Di, X. M. Liu, Y. Shao, B. F. Ma, J. H. Lee, K. S. Ha, *Stem Cells* **2010**, *28*, 2162.
[35] B. L. MacInnis, R. B. Campenot, *Science* **2002**, *295*, 1536.
[36] J. D. Whittle, D. Barton, M. R. Alexander, R. D. Short, *Chem. Commun.* **2003**, 1766.